



The anthropogenic influence on the estuarine system of Gosaba Island, Sundarban, India

Soumen Ghosh¹ · Biswaranjan Mistri¹

Received: 16 February 2021 / Accepted: 11 August 2021 / Published online: 25 August 2021
© Saudi Society for Geosciences 2021

Abstract

The spatial pattern and morphological characteristics of creek channels have been altered due to anthropogenic interferences such as the construction of embankment, erection of closures and unsystematic human encroachment on drainage channels of Gosaba Island. The saucer-like appearance of the island and the deterioration of drainage channels have adverse impacts on the estuarine environment. To address these issues, this study highlights the spatial pattern and morphological change of drainage channels and illustrates their negative impacts on Gosaba Island. In this study, US Army Toposheet of 1955, multi-temporal Landsat data from 1972 to 2017, ALOS-PALSAR DEM, high-resolution Google Earth images, and cadastral maps were incorporated in remote sensing and GIS environment to assess the drainage density, morphological characteristics of creeks, spatial risk of flood inundation, and proximity analysis of households along the drainage channels. Furthermore, the direction of surface slopes was measured by instrumental surveying, as well as collecting a variety of information about drainage congestion and the resulting problems during field surveys. The study revealed that channel decay, the morphological changes in creek characteristics, and embedded drainage systems are increasing the risk of flood inundation and waterlogging problems in the agricultural field, especially in times of natural calamity. For the future sustainability of Gosaba, the government must take control over the imprudent human interventions on the drainage system.

Keywords Creek channels · Anthropogenic influence · Drainage decaying · Waterlogging · Flood inundation

Introduction

A part of the Gangetic delta, the Sundarban delta is spread over both India and Bangladesh (O'Mally 1914; Allison 1998; Rahman et al. 2020). The delta was formed through the deposition of alluvium from the Ganga and Brahmaputra Rivers and is characterized by an intrinsic network of tidal creeks (Banerjee 1998; Haldar and Debnath 2014; Ghosh and Mistri 2020a). Tidal creeks are linked to major rivers and are interconnected (Ghosh and Mistri 2020b). The Sundarban creeks are navigable for almost 10,000 km

(Rogers et al. 2014). The drainage network of the delta is very complex. This riverine system is very sensitive to climatic disasters due to imprudent anthropogenic activities such as human encroachment at the creek estuary, land-use modification, unsystematic construction of embankments, and erection of several barriers across drainage channels (Zhao et al. 2019). The morphology of tidal creeks is influenced by wave action, diurnal tidal activity, surface runoff processes, flow variability, and topography. It is considered that these creek channels and the surrounding marshy lands are potential nursery grounds for fish (Boesch and Turner 1984). Therefore, these drainage channels are often divided into several micro water compartments by local inhabitants specifically for year-round fisheries and irrigation purposes in the dry season (Ghosh and Mistri 2020b). As a result, creek channels are slowly defunct with time by this inconsiderate human activity (Mistri 2014; Ghosh and Mistri 2020b, c). Tidal creeks play an important role in the formation of deltas (Allison 1998). While the average elevation of the delta is almost 3m above mean sea level, the wave height of recent environmental extremes often exceeds over 5m (Rudra 2016). At Sagar Island, sea level rise

Responsible Editor: Stefan Grab

✉ Soumen Ghosh
ghoshsoumen864@gmail.com

Biswaranjan Mistri
brmistri@gmail.com

¹ Department of Geography, The University of Burdwan, West Bengal 713104, India

was around 2.6 mm/year because of subsidence factors (Gopinath and Seralathan 2005), which was higher than the global rate of sea-level rise (SLR) of 1.7 to 1.8 mm/year during the twentieth century (Holgate and Woodworth 2004; Church et al. 2006; Jana et al. 2013). Tropical cyclones in Sundarbans are becoming more frequent and more severe due to SLR and warming sea surfaces over the North Indian Ocean (Khan et al. 2000; Agrawala et al. 2003). In times of storm surge-induced flooding, this situation can be quite miserable for local people because of mismanagement of the drainage system (Hazra et al. 2002; Ghosh and Mistri 2020b). Land reclamation began in Sundarbans by the construction of embankments and erection of closures during the 18th century mainly to prevent saline water intrusion into agricultural land (Ghosh and Mistri 2020a; Ghosh et al. 2015). Consequently, the normal functioning of the drainage system has been adversely affected (Mistri 2014; Ghosh and Mistri 2020c). As a result of human encroachment on drainage channels, patterns, alignment and interconnectivity of drainage networks have been drastically altered (Sanyal 1999; Mistri 2014). Many of the drainage channels are slowly disconnected from their source rivers and gradually decaying (Bhradra et al. 2017; Ghosh and Mistri 2020a, b). As a result of this embedded drainage system, this island is vulnerable to flood hazards and disasters (Ghosh and Mistri 2020b).

Remote sensing and GIS have recently been used to study the changing pattern of tidal creeks in deltaic environments (Shi et al. 1995; Liu et al. 2013). In previous research, Chust et al. (2008) and Zhao et al. (2019) have used a 3D terrain model using light detection and ranging (LiDAR) to effectively understand the morphological characteristics of tidal creeks. Based on field investigations and hydrological experiments, scientists have assessed morphometric parameters of creeks (Tambroni et al. 2005; Stefanon et al. 2010; Fagherazzi et al. 2012; Kim et al. 2013). Williams et al. (2002) conducted a cross-sectional survey of tidal creeks on the marshy island to study their formation and development. Some researchers, on the other hand, have used morphometric attributes to examine the formation of creeks in estuaries (Marani et al. 2003; Novakowski et al. 2004; Seminara et al. 2010; Davies and Woodroffe 2010; Hood 2010). Therefore, the physical parameters studied over the years have provided a broad insight into the temporal evolution of tidal creeks. Compared to other parts of the world's delta, the Indian Sundarban delta has not received widespread attention. In this delta, the tidal network has been intensively modified due to anthropogenic interferences and this modification has adversely impacted the estuarine environment for the long term, especially in regards to flood control, which has been overlooked by previous researchers. To fulfill these research gaps, the present research work at first highlighted the morphological attributes of creeks and changing pattern of drainage networks due to human interventions over the years. Further, this study also elaborates

on various negative implications of a mismanaged drainage system on the deltaic environment. The present study helps to understand the future threats to the delta from defective drainage systems and encourages coastal planners to develop drainage management plans to make the delta more resilient.

The study area

The Indian Sundarban delta is low lying, tidally active (tidal range is >4m), in the northern part of the Bay of Bengal (Ghosh and Mukhopadhyay 2016). During the 10000-3000 cal year BP period, the delta was formed (Goodbred and Kuehl 2000; Allison et al. 2003; Bhadra et al. 2017). This delta's unique geomorphology is characterized by an alluvial plain, meandering channels, salt marshes, and mangrove swamps that are dissected by an intrinsic drainage system. In Sundarbans, mangrove forests have declined by nearly 40% in the last 300 years due to human exploitation (Islam et al. 1997; Rogers et al. 2014). This delta witnessed massive deforestation during the 1770s as a result of land reclamation (Pargiter 1934; Sarkar et al. 2016; Danda et al. 2017). The vast mangrove forest of Sundarban was partially cleared by the British rulers with the help of local landlords to increase the revenue collection from reclaimed agricultural land (Dutta 2014; Halder and Debnath 2014). The reclamation in Gosaba Island (21°54'N to 22°08' N and 88°29'E to 88°49'E) was initiated by Sir Daniel Hamilton, a Scottish businessman who leased 9000 acres of land (lots 143 and 149) and constructed earthen embankments along the rivers to protect agricultural land (Dutta 2014). In 1909, there were only 900 residents on this island (Dutta 2014). However, after India's independence, the population of Gosaba Island has gradually increased. According to the latest census archived data for 2011, a total of 246598 people live on this island over an area of 296.43 km² (Census of India 2011). In 2001-2011, the estimated population density was about 830 people per km² and the population growth rate was about 10.7% (Census of India 2011). The Bidya River borders the island on the west and Gomar and Raimangal Rivers on the east. Tidal amplitudes range from 2m to 4m on Gosaba Island when extreme weather events occur (Brown and Nicholls 2015). The mean annual rainfall varies from 180 cm to 200 cm and 80% of the annual rainfall occurs in the monsoon season (June to October). The island has been periodically affected by tropical cyclones, floods caused by storm surges and embankment breaching. The Gosaba Island consists of 14 Gram Panchayats (GPs), the local self-government system in India in accordance with the Panchayati Raj which includes Amtali, Bali I and II, Bipradaspur, Chhota Mollakhali, Gosaba, Kachukhali, Kumirmari, Lahiripur, Pathankhali, Rangabelia, Radhanagar-Taranagar, Satjelia and Sambhunagar and 50 villages inhabited (Fig. 1).

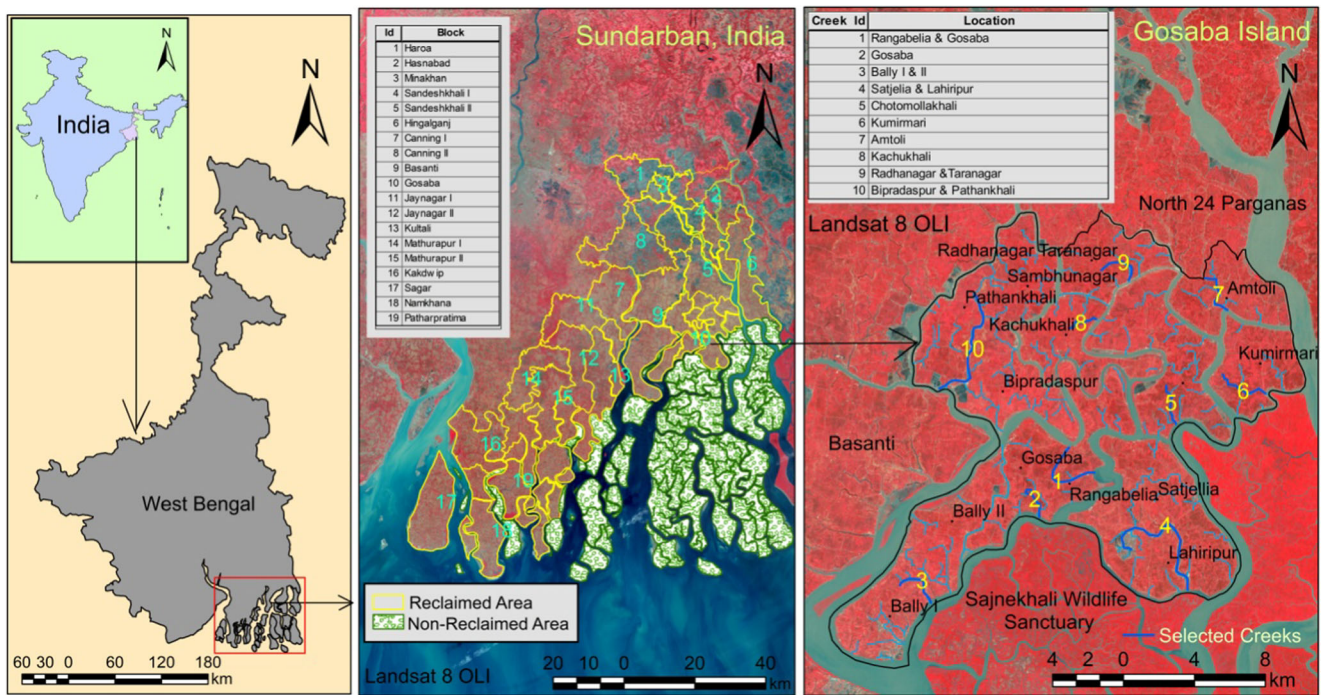


Fig. 1 Location of the study area

Materials and Methods

In the present study, different multi-temporal post-monsoon period Landsat images such as Landsat MSS (spatial resolution 60m) data for the year 1972 and 1980, Landsat TM (spatial resolution 30m) data for the years 1997 and 2010 and Landsat 8 OLI data (spatial resolution 30m) for the year 2017 were used for the spatial analysis (Table 1). As the spatial resolution of the Landsat data differs, the Landsat MSS

data were considered in this study as the base image and these images (Landsat MSS 1972 & 1980) were resampled applying bilinear interpolation resample technique to match the spatial resolution with Landsat TM and Landsat 8 OLI data. Thereafter, the top-of-atmosphere (TOA) reflectance was calculated to avoid the sensor spectral radiance. The exoatmospheric TOA reflectance helps to improve the quality and interpretability of remotely sensed data. The TOA reflectance of the earth was calculated using Eq. 1 as used by

Table 1 Description of detailed data sets

Data Sets	Description	Pixel Size	Date of Acquisition	Path and Row	Source
Satellite Data	Landsat MSS	60m*	05-Nov-1972	148 & 45	United states geological survey (USGS) https://earthexplorer.usgs.gov
	Landsat MSS	60m*	17 Nov 1980	148 & 45	
	Landsat TM	30m	01 Nov-1997	138 & 45	
	Landsat TM	30m	23 Nov-2010	138 & 45	NRSC, Bhuban http://bhuvan.nrsc.gov.in/data/download/index.php
	Landsat 8 OLI	30m	08-Nov-2017	198 & 45	
	LISS III	23.5m	25-Nov-2011	108 & 56	
Digital Elevation Model (DEM)	ALOS PALSAR	12.5m	13-July-2008	506 & 430	Alaska Satellite Facility https://vertex.daac.asf.alaska.edu/
US Army Toposheet	Toposheet No. NF-45-08	Scale 1:250,000	Year of Compilation 1955	Source www.lib.utexas.edu	

*Resampled resolution 30m

Chander et al. (2009); Li et al. (2013) and Bhadra et al. (2017).

$$\rho_{\lambda} = \frac{\pi \cdot L_{\lambda} \cdot d^2}{ESUN_{\lambda} \cdot \cos \theta_s} \quad (1)$$

Where ρ_{λ} denoted planetary TOA reflectance [unitless], d^2 is the earth-sun distance [astronomical units], π is the mathematical constant equal to ~ 3.14159 [unitless], $ESUN_{\lambda}$ is the average atmospheric solar irradiance [Watts/(m²* μ m)], θ_s is the solar zenith angle [degree] and L_{λ} is the spectral radiance at the sensor's aperture [Watts/(m²*ster* μ m)]. The L_{λ} is calibrated using the following Eq. 2.

$$L_{\lambda} = \left(\frac{LMAX_{\lambda} - LMIN_{\lambda}}{Q_{cal\ max} - Q_{cal\ min}} \right) (Q_{cal} - Q_{cal\ min}) + LMIN_{\lambda} \quad (2)$$

Where $LMIN_{\lambda}$ is the spectral at-sensor radiance that is scaled to $Q_{cal\ max}$ [W/(m² sr μ m)], $LMIN_{\lambda}$ is spectral at-sensor radiance that is scaled to $Q_{cal\ min}$ [W/(m²*sr* μ m)], $Q_{cal\ max}$ is the maximum quantized calibrated pixel value corresponding to $LMAX_{\lambda}$ [DN], $Q_{cal\ min}$ is the minimum quantized calibrated pixel value corresponding to $LMIN_{\lambda}$ [DN], and Q_{cal} is the quantized calibrated pixel value [DN].

Thereafter, two different water index methods namely McFeeters's Normalized Difference Water Index (NDWI) and Xu's Modified Normalized Difference Water Index (MNDWI) were adopted to enhance the spectral signal reflected from water bodies and removed various noise components of other wavelength regions (Xu 2006; Ji et al. 2009; Li et al. 2013). McFeeters's NDWI formula is shown in Eq. 3.

$$NDWI = \frac{\rho_{Green} - \rho_{NIR}}{\rho_{Green} + \rho_{NIR}} \quad (3)$$

Where ρ_{Green} and ρ_{NIR} shows the reflectance of the green band and near-infrared band.

NDWI cannot effectively distinguish build-up areas from water bodies. This limitation is overcome by using Xu's MNDWI model to identify open water features from satellite images. According to Xu, MNDWI is delineated using Eq. 4.

$$MNDWI = \frac{\rho_{Green} - \rho_{SWIR}}{\rho_{Green} + \rho_{SWIR}} \quad (4)$$

Where ρ_{Green} and ρ_{SWIR} is the reflectance of the Green and SWIR band. Finally, the MNDWI model is used in this study for better visual contrast between land-water pixels.

In this study, ERDAS IMAGINE 2014 software was used for image processing, radiometric correction and enhancement. Besides, ArcGIS 10.8 software was chosen for resampling of satellite data, digitalization and mapping purposes. The projection system was used in this study Universal Transverse Mercator (UTM) with WGS 1984 datum and the UTM zone 45N. The detailed methods used in this study have been elaborated in the following sub-headings.

Delineation of creek parameters

Based on visual analysis of satellite images, ten major creek channels were selected from different parts of Gosaba Block, where the greatest temporal change and modification of creek channels have been observed in the recent decades (Table 2). These channels were categorized based on estuary characteristics. Estuaries are considered 'open' if there is a free flow of water and sediment from rivers to tidal creeks as a result of tidal effects. A 'closed estuary' is one in which the free flow of sediment and water is restricted by various human-induced obstructions across the channel. To minutely observe the spatiotemporal change of creek channels, radiometrically corrected and model output enhanced satellite images were incorporated in the GIS environment. It helps to delineate various parameters such as creek width, length, perimeter and water surface area. To measure the width of a creek channel, three segments were measured: mouth, middle, and tail. The 'mouth' of a creek is where it meets a river. 'Middle' is the centre of the entire length of a creek. 'Tail' refers to the landward last zone of a creek (Ijaz et al. 2018). A tidal creek's perimeter is the geometric extent of the creek from mouth to tail, measured for the period of 1972- 2017. GIS software has been used to digitize the centerline of each creek which is the exact middle point of the delineated bank lines to obtain each creek's length (McSweeney et al. 2017; Ijaz et al. 2018). These measurements were done using the measurement tool in ArcGIS 10.8 (Fig. 2). For understanding the changes in the channel planform over time, the sinuosity of selected creeks was calculated using Eq. 5 (Leopold and Wolman 1957).

$$\text{Sinuosity} = \frac{\text{Meandering length}}{\text{Valley length}} \quad (5)$$

Based on the sinuosity index (SI), tidal creeks were classified into three categories *i.e.* straight (SI < 1.05), sinuous (SI 1.05-1.5) and meandering (SI > 1.5).

Extraction of the drainage network

The drainage network was extracted from the US Army Toposheet of 1955, Landsat MSS of 1972 and Landsat 8 OLI 2017 to overview the spatiotemporal changing pattern of the drainage system. Each creek was digitized using the polyline feature from the topographical sheet and selected satellite images. To compare the temporal changes in lateral connectivity of the drainage network, overlay analysis was conducted. The spatial density of the drainage network was determined using the line density tool in ArcGIS. Thereafter, drainage density was calculated using the zonal statistics tool in the GIS platform to study the spatial and temporal changes.

Table 2 Geographical details of selected creeks

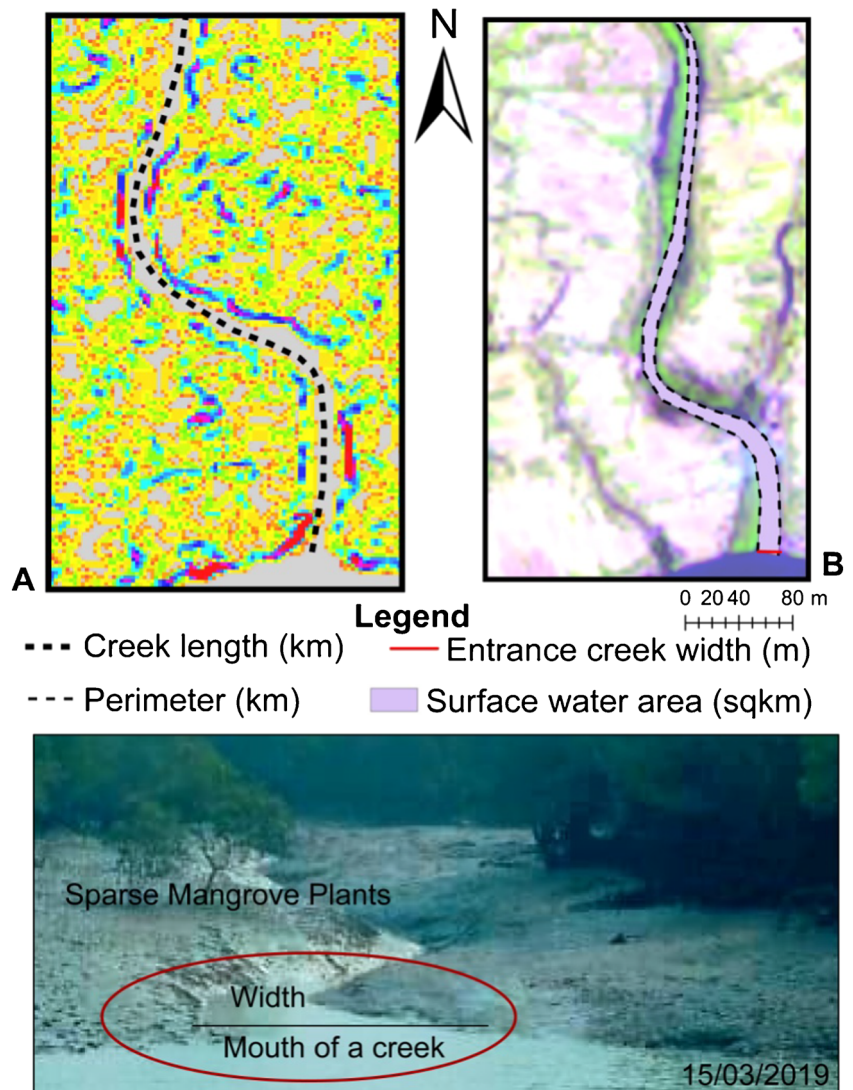
Creek No.	Latitude	Longitude	GP Name	Type of estuary
1	22°09'02"	88°50'30"	Rangabelia and Gosaba	Closed estuary
2	22°07'58"	88°48'58"	Gosaba	Open estuary
3	22°05'17"	88°45'13"	Bally I and II	Closed estuary
4	22°05'29"	88°53'45"	Satjelia and Lahiripur	Open estuary
5	22°10'33"	88°53'25"	Chotomollakhali	Open estuary
6	22°11'26"	88°56'20"	Kumirmari	Closed estuary
7	22°14'05"	88°55'00"	Amtoli	Closed estuary
8	22°13'45"	88°50'49"	Kachukhali	Closed estuary
9	22°14'57"	88°51'56"	Radhanagar and Taranagar	Closed estuary
10	22°11'57"	88°46'08"	Bipradaspur and Pathankhali	Closed estuary

Proximity analysis

The settlement pattern on Gosaba Island is linear, concentrated along rivers or creek channels, primarily for irrigation and

communication. For a better understanding of the human activity surrounding the creek channels, a proximity analysis was done in the GIS platform using the high-resolution Google Earth image, while cadastral maps compiled from

Fig. 2 Example of assessing various morphological parameters of creeks



the Gosaba panchayat office were used to verify the results. Initially, Google Earth images of the study area were saved in their maximum resolution (4800×2722) and imported into the ArcGIS environment for georeferencing and image mosaicking. Thereafter, multiple buffer layers were created from the selected creeks using the geoprocessing tool. The shapefile layer of point feature was generated to identify every single household within the specified buffer zone and each buffer zone's household density was determined by using the point density tool. For example, the household proximity analysis of creek Id 4 is shown in Fig. 3.

Calculation of land transformation

During the assessment, the land transformation was seen mainly as a consequence of the water area becoming land. For this study, multi-temporal vector boundaries were superimposed for two consecutive years (1972 & 1997, 1997 & 2017), and the area of conversion was then delineated using the ArcGIS measurement tool. To check the accuracy level, the pixel-based spectral reflectance curve of the Near Infra-Red (NIR) band of Landsat images (band 3 for Landsat MSS, band 4 for Landsat TM and band 5 for Landsat 8 OLI) were used to avoid confusion regarding mixed pixels. A trough in the spectral reflectance curve of the NIR band indicates the presence of water pixels, while a sharp peak indicates

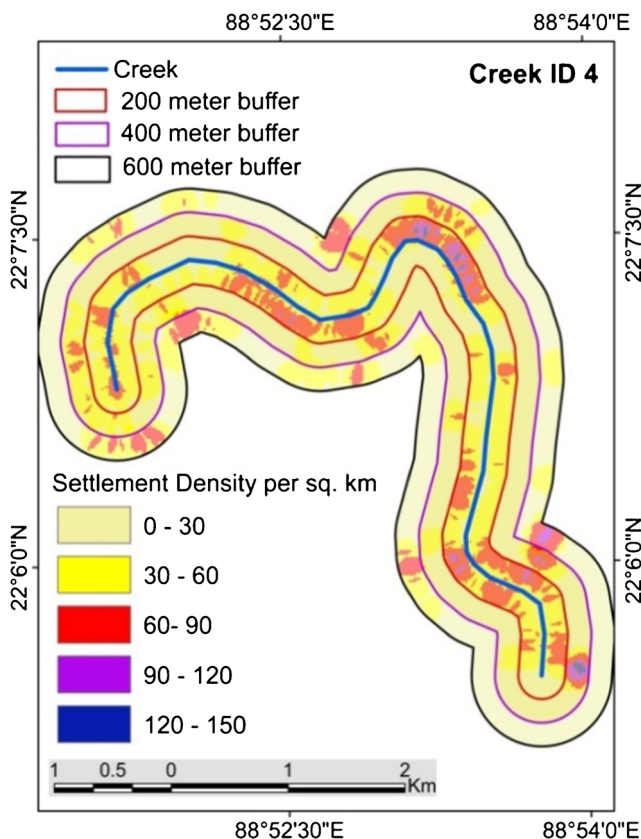


Fig. 3 A proximity analysis of households along a creek channel

the absence of water pixels. Further, field verification was carried out at some specified locations to validate the results and improve the accuracy level of the work.

Flood inundation modeling and field surveying

The study area is highly flood-prone. It was observed during the field survey (2017-2018) that at various locations, the bank height was <1 m. The storm surge height during extreme climatic events was recorded to be 2m-4m higher than the astronomical tide in the last 20 years (Kar and Bandyopadhyay 2015; Sakib et al. 2015; Gayathri et al. 2015). Therefore, the spatial flood inundation model was prepared taking into account the 3m storm surge during severe cyclone Aila on 26 May 2009 (www.storm-surge.info). To calculate the flood inundation, Advanced Land Observing Satellite-Phased Array type L-band Synthetic Aperture Radar (ALOS-PALSAR) Digital Elevation Model (DEM-12.5m spatial resolution) was used. Recently, the gravity correction was applied by various scholars before processing SAR DEM data for spatial modeling (Das et al. 2015; Bandyopadhyay et al. 2021). The pixel-level ellipsoidal heights of SAR DEM data were converted into orthometric heights in PCI Geomatica 2015 environment by subtracting geoidal elevation which was obtained from the Earth Gravity Model of 2008 (Pavlis et al. 2012). The permanent water bodies were identified from the MNDWI model output and excluded from DEM. To identify the flood-affected areas under the specified flood inundation limit, a GIS-based special flood routing algorithm was used.

Instrumental surveying to determine the slope direction and preparation of land use map

The dumpy level survey was conducted in a micro plot of the Gosaba mouza to determine the slope direction change along creeks using a GPS receiver to collect XY coordinates (X-longitude and Y-latitude). The average ground elevation was considered 2m above the mean sea level collected from Gosaba Irrigation Sub-Division Office for surveying. GPS recorded the XY coordinate when the precision level was <3m. The Z value of that particular point was a representation of the surface elevation as measured by the Dumpy level. In order to interpret the change of elevations and slopes in such flat land, instrumental surveying was conducted, as it gives a more precise result than using DEM. The Reduced Level (RL) was calculated using the collimation method in this study. The obtained XYZ data were then incorporated into the ArcGIS environment. Next, a DEM was produced using a spatial analyst tool and a contour map was also generated from the DEM to identify the gradient change.

Georeferenced Google Earth images (US Dept. of State Geographer, Imagery date 12/8/2018) and cadastral map

(Gosaba mouza, Gosaba, Scale-1:2500, Source: Gosaba Panchayat Office) of the surveying plot were used to compile a land-use map demonstrating the relationships between land use types and slopes. In the assessment of horizontal accuracy of the high-resolution Google Earth image (RMSEr), 4.2m is shown (Mean 3.4m; SD 2.3m) from the available images from 2008 onwards. Therefore, it is quite reliable for scientific research (Paredes-Hernandez 2013). Based on the Federal Geographic Data Committee's RMSEr formula, Eq. 6 was used for calculating RMSEr (Federal Geographic Data Committee (FGDC) (USA) 1998).

$$\text{RMSE}_x = \sqrt{\frac{\sum_i (x_{\text{data},i} - x_{\text{reference},i})^2}{n}} \quad (i)$$

$$\text{RMSE}_y = \sqrt{\frac{\sum_i (y_{\text{data},i} - y_{\text{reference},i})^2}{n}} \quad (ii)$$

$$\text{RMSE}_r = \text{RMSE}_x^2 + \text{RMSE}_y^2 \quad (iii)$$

$$(6)$$

Where, $x_{\text{data},i}$, $y_{\text{data},i}$ are the co-ordinates of the i^{th} point in the evaluated dataset, $x_{\text{reference},i}$, $y_{\text{reference},i}$ are the co-ordinates of the i^{th} point in the independent reference dataset of higher accuracy, 'n' is the number of checkpoints; 'i' is an integer that ranges from 1 to n.

Field survey

To observe the ground problem of drainage congestion, a transect walk was carried out in different parts of Gosaba block especially in Rangabelia, Bipradaspur, Bally I and Bally II GP during both monsoon and dry seasons (2017-2018). The whole collection of more than 50 photographs was captured during the monsoon season (10th July 2017 to 25th July 2017) and the post-monsoon season (25th December 2017 to 21st January 2018). For the purpose of this study, suitable and best photographs were then selected. Moreover, primary information on drainage congestion and the resulting water inundation problem was also collected through face-to-face interviews with more than 100 respondents aged over 40 years old and engaged in agriculture and pisciculture activities.

Results and discussion

To study the change of morphological characteristics of creek channels at the human-nature interface from 1972 to 2017, various parameters have been selected and discussed accordingly in the following sections.

Morphological characteristics of creek channels

Spatiotemporal variation in creek width

The entire delta is crisscrossed by several creeks and rivers. Since the 19th century, these creeks have been intensively modified and gradually encroached by human activities. As a result, the width of creeks has been declining over time and the channels have been getting narrower (Fig. 4). The average creek width measured in 1972 was 170.90m, then 86.40m in 1997, and 58.50m in 2017. In the middle section, the average width decreased from 145.40m in 1972 to 43.90m in 2017. The width of the creek towards the tail abruptly decreased from 107.10m in 1972 to 27m in 2017 as a result of land transformation. The width of the channel varies according to the estuary type. Those creeks that have a direct connection to their source have the maximum width, and those creeks that have been disconnected from the parent river due to anthropogenic obstructions have the minimum width. A tidal creek characterized by an open estuary is highly influenced by the hydrodynamic processes of the river. Tidal waters and floods frequently inundate the land adjacent to these kinds of creeks. During the field survey, it was found that the number of lock gates was not sufficient and protective enough to control flooding on this island. The unplanned construction of the embankment often obstructs the water circulation system and the situation becomes worrisome in the case of a closed estuary. Due to a defective water circulation system, prolonged waterlogging in inland agricultural land becomes inevitable.

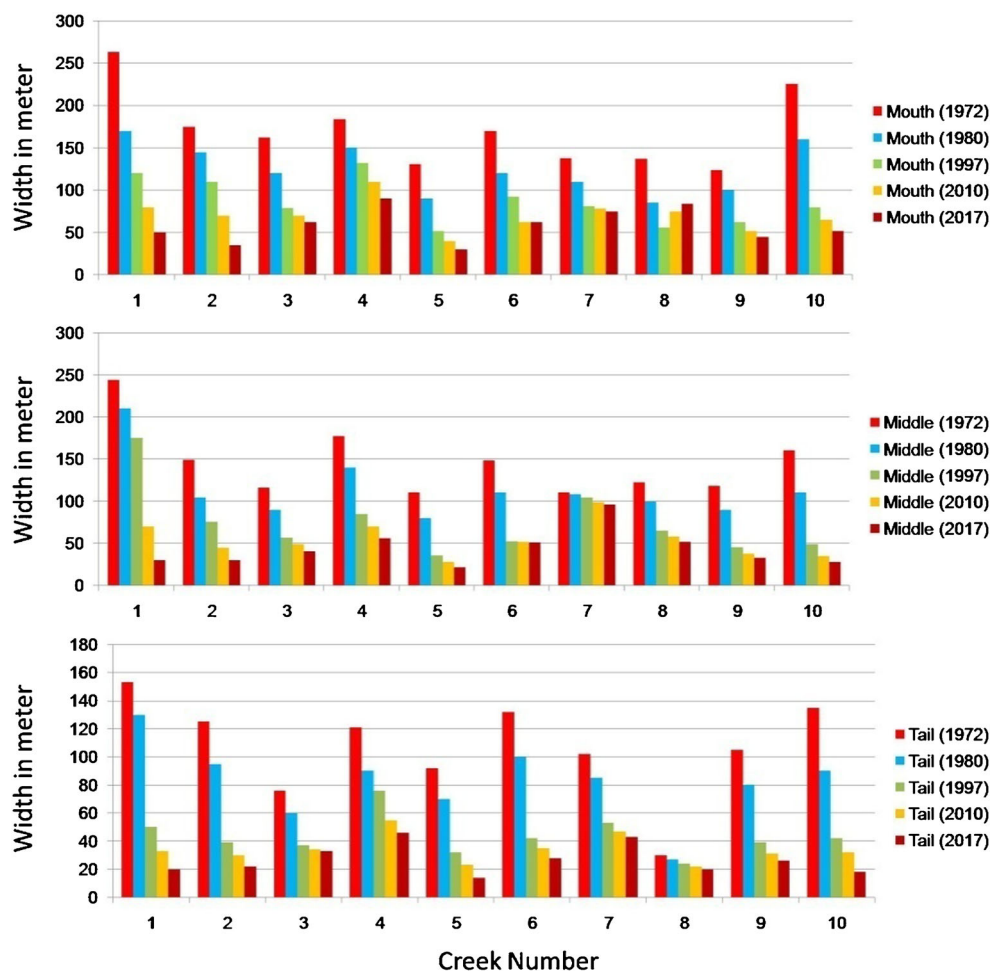
Changes in creek length and perimeter

The length and perimeter of creek channels are correlated to each other. This analysis revealed that the length and perimeter of the selected creeks are gradually decreasing over the years. The average length and perimeter of these creeks were measured at almost 3.87 km and 8.33 km respectively in 1972. The length was reduced up to 2.91 km and the perimeter decreased up to 5.7 km in 2017. There was a positive correlation ($r = 0.72$) found between the decreasing trend of creek length and perimeter (Fig. 5).

Temporal variations in creek length and sinuosity

Due to natural and anthropogenic factors, the sinuosity of tidal creeks is slowly changing over time. In relation to the decrease of creek length during 1972-2017, the average sinuosity changed from 1.51 to 1.21 (Fig. 6). Meandering channels are gradually becoming sinuous. Local dwellers have partially encroached on these creeks for primary activities, converting

Fig. 4 Spatiotemporal changes in creek width (1972-2017)



them into ‘rayot’ land for temporary purposes. This leads to a gradual disappearance of these creeks over time.

Variation in water surface area of creeks

As each creek's width, length, and perimeter reduced, the water surface area decreased as well. In 1972, the average water surface area was 0.56 sq. km, which has since decreased to 0.13 sq. km. km in 2017 (Table 3). The water area has been shrinking over the last four decades due to a shortage of water supply from its source river. Creek channels gradually decay with time due to human-induced intermittent obstructions, such as closures, fisheries, and encroachments.

Temporal conversion of land characteristics

The conversion of creek areas into ‘rayot’ (personal land) and community land is common on this island. Land conversion intensified during the land reclamation process and again during the land reform movement in the 1980s known as ‘Operation Barga’ in West Bengal. The goal of this movement

was to redistribute land ownership in favour of the cultivators (Bandopadhyaya 1981). Therefore, during 1972-1997, the rate of land conversion was estimated to be quite high (7.37 ha) in comparison to 1997-2017 (5.03 ha) (Table 4). A positive correlation ($r = 0.74$) was found between the rate of land gain through land conversion and the change in creek perimeter during the period 1972-2017 (Fig. 7).

Changing pattern of the drainage network

Prior to land reclamation, Gosaba Island was covered with dense mangrove forests and had an intrinsic drainage system. Due to rapid population growth and human activities, lateral connectivity of the drainage system is gradually decreasing. During 1955-2017, the drainage area decreased from 38% to 18% (Fig. 8). During 1955-2017, the drainage density of Gosaba Island decreased from 1.75 km/sq. km to 0.91 km/sq. km. Channel decay is indicated by a negative change in drainage density. This was estimated relatively high in Gosaba GP (−0.35), Bally I GP (−0.54), Chotomollakhali GP (−0.70), Lahiripur GP (−0.71) and Bipradasur GP (−0.49).

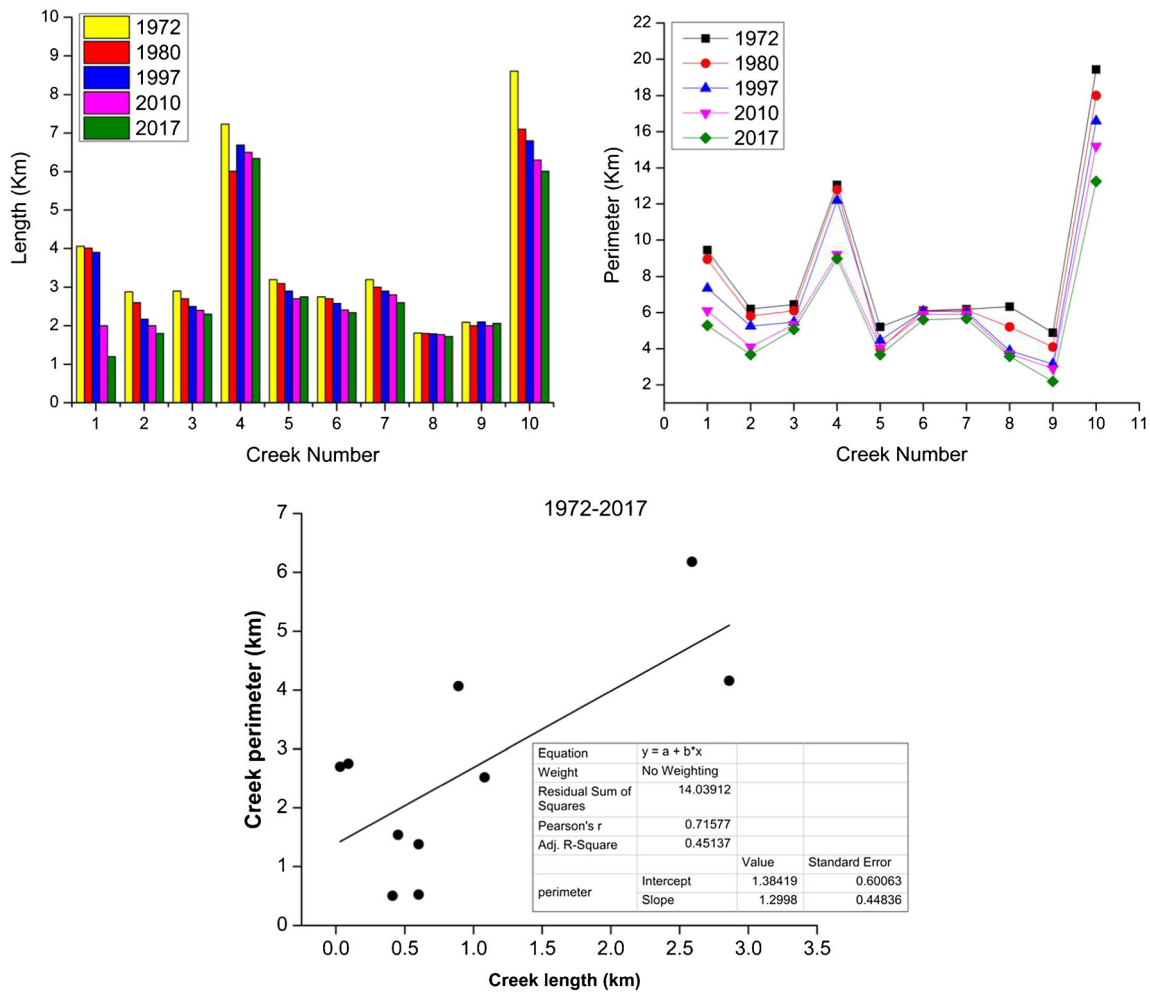


Fig. 5 Variations in creek length and perimeter (1972-2017)

Underlying causes responsible for spatiotemporal change of creek morphology in the study area

(a) Human habitation was made possible on this island by clearing dense mangrove forests and constructing

embankments along the rivers. The construction of embankments has resulted in siltation within drainage channels. Therefore, channel depth is gradually decreasing over time (Sánchez-Triana et al. 2018). Residents have occupied the estuary zones of several creeks and gradually disconnected themselves from the source rivers. During the field survey, it

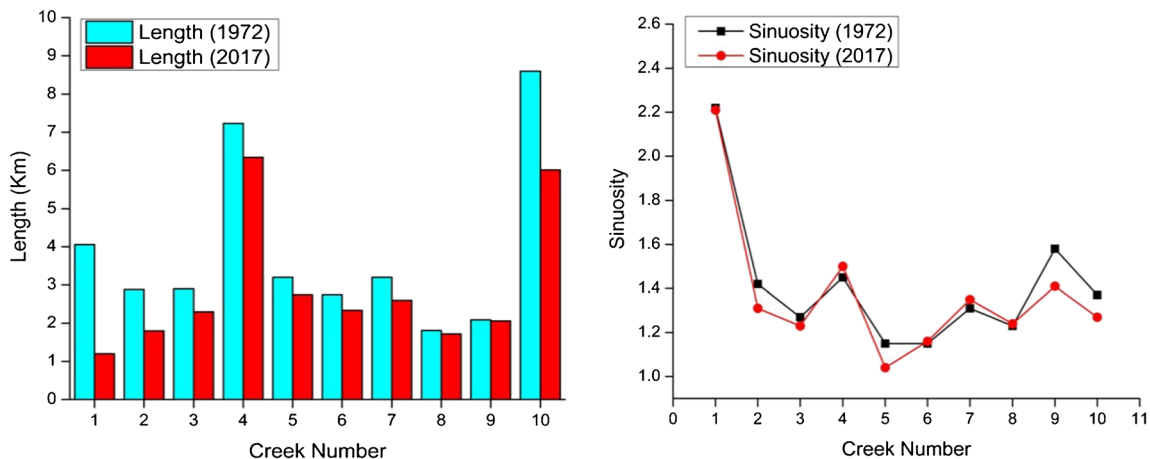


Fig. 6 Variations in creek length and sinuosity (1972-2017)

Table 3 Change in water surface area from 1972 to 2017

Creek Id	1972 (sq. km)	1980 (sq. km)	1997 (sq. km)	2010 (sq. km)	2017 (sq. km)	(1972-2017) (sq. km)
1	0.73	0.56	0.31	0.19	0.11	-0.62
2	0.39	0.23	0.12	0.10	0.08	-0.31
3	0.36	0.22	0.13	0.12	0.11	-0.25
4	1.25	0.95	0.68	0.53	0.46	-0.79
5	0.29	0.19	0.07	0.06	0.05	-0.22
6	0.37	0.21	0.13	0.10	0.09	-0.28
7	0.33	0.29	0.24	0.21	0.18	-0.15
8	0.29	0.23	0.11	0.09	0.07	-0.22
9	0.36	0.25	0.08	0.05	0.03	-0.33
10	1.31	1.01	0.32	0.20	0.11	-1.20

was noted that the main settlement and the market of Gosaba were developed adjacent to a creek estuary. A number of creeks, or what locals called 'khals,' were used for fishing and farming. These creeks were divided into several micro water ponds for storing water and used for daily livelihood activities. Furthermore, road constructions, dumping of garbage, and unauthorized construction activity have impacted the overall fluvial system of the delta (Fig. 9). The morphological characteristics of creeks have been modified by human interventions and are slowly deteriorating.

(b) In Gosaba Island, linear settlements were initially developed along drainage channels for easy access and communication. Since the British colonial period, these creeks have been an important means of communication between islands. The GP level study found a negative correlation ($r = -0.57$) between population growth (2001-2011) and drainage densities. The buffer analysis was conducted to estimate the anthropogenic pressure on these creeks. Analysis revealed that the average density of households within the 200m buffer zone was 70 households per sq. km, which was four times higher than the next buffer zone (18 households per sq. km) and seven times higher than the outer buffer zone (9 households

per sq. km) (Fig. 10). Due to the excessive concentration of settlements surrounding creeks, the drainage system is subjected to heavy anthropogenic pressure.

(c) Conflict between 'rayot' lands and community lands is a great challenge for drainage system management. Local people often partially modify drainage channels for their benefits as well as community interests without assessing their future effects on riverine systems. In the course of time, the intermittent construction of closures across creek channels obstructs the free flow of water and causes the decay of creeks.

Impact of anthropogenic influence on the estuarine system

Change of slope direction

Several embankments and closures have been constructed across these creeks, increasing sedimentation. During the

Table 4 The rate of land transformation from 1972 to 2017

Creek ID	1972-1997 (ha)	1997-2017(ha)	1972-2017 (ha)
1	9.29	7.56	16.85
2	8.84	4.23	13.07
3	5.81	4.14	9.95
4	15.19	11.56	26.75
5	6.32	3.25	9.57
6	4.56	3.19	7.75
7	4.12	2.96	7.08
8	3.75	2.59	6.34
9	5.29	3.54	8.83
10	10.62	7.29	17.91

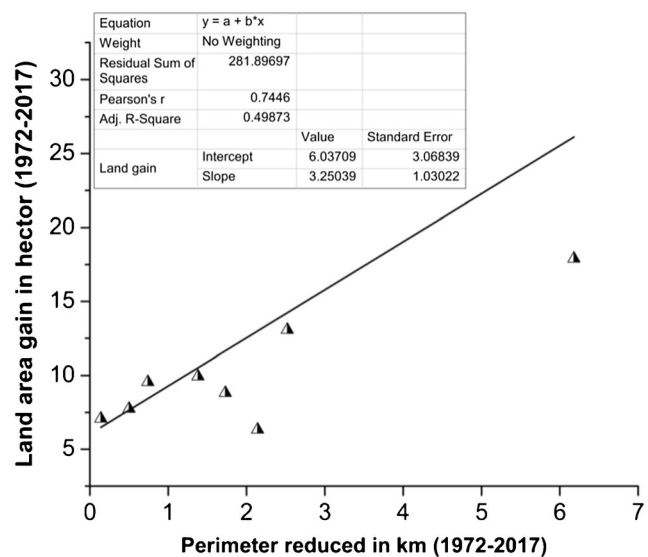
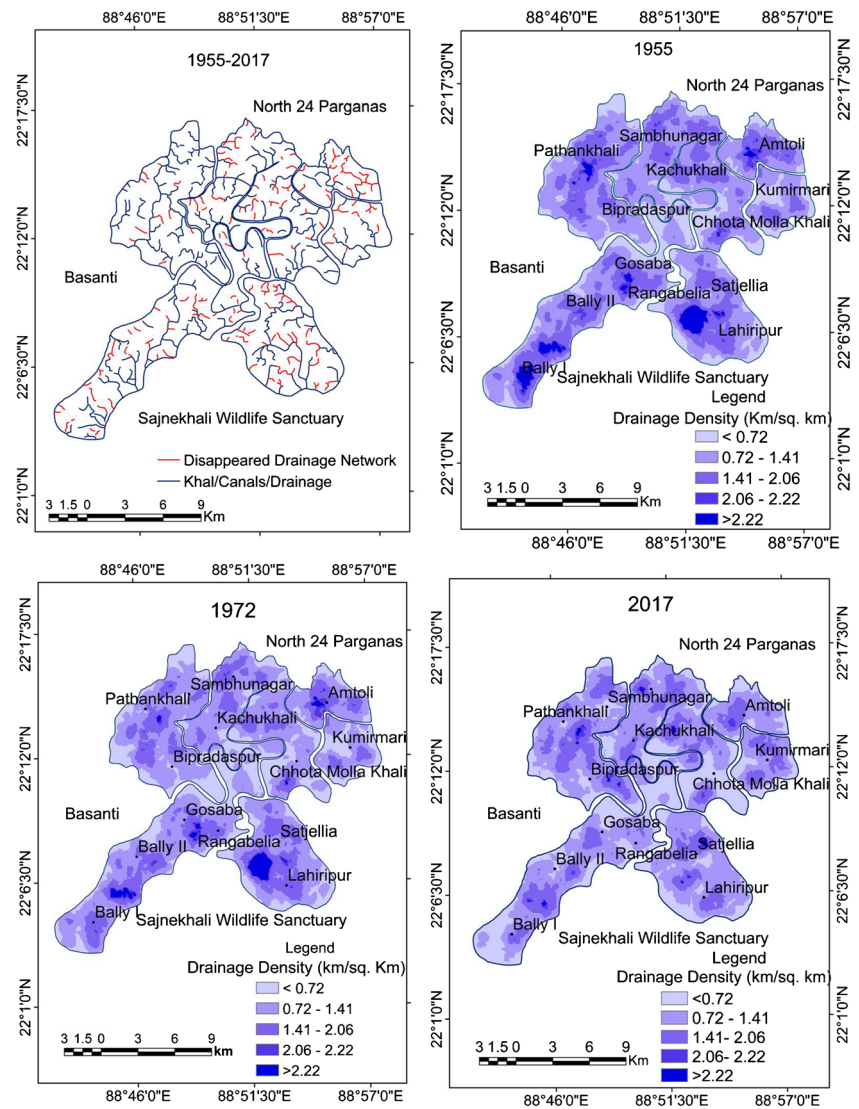


Fig. 7 Correlation between land gain and change in creek perimeter

Fig. 8 Spatiotemporal change of the drainage network during 1955-2017



monsoon season and environmental extremes, excessive water from drainage channels often floods adjoining land, causing siltation in the floodplain area, compared to the inward land. This inward land appears as a saucer shape and water accumulated over a long time. To study the change of surface slope direction along the drainage channels, a small plot of the Gosaba island (36.74 ha) was surveyed and a land-use map was also prepared of that part to understand the dominance of cultural landscape over natural entities (Fig. 11). Based on the derived land use map, it is evident that various human activities surround drainage channels. These channels are converted into small ponds for their personal use as shown in the land use map. The a-b cross-section line on the land use and elevation map clearly illustrates how the gradient of the land is gradually decreasing from the drainage channels to the inward land. As a result, inwardly saucer-shaped agricultural land is

quite difficult to drain and farmers are facing acute problems of waterlogging.

Risk of flood inundation in the coastal region

The average elevation of the island remains below the high tide line. The choking of drainage channels and resulting drainage congestion poses a serious threat to the island, especially to the farmers. Construction of closure at the creek estuary prevents the free flow of water. Therefore, countryside water may not drain out properly into the main river via the inland drainage system. The survey revealed the height of the embankment from the high tide line in various places was less than 1m. Accordingly, if the water level rises >3m as reported during severe cyclone Aila in 2009 and Amphan in 2020, the maximum area of Gosaba Island will be flooded as shown in

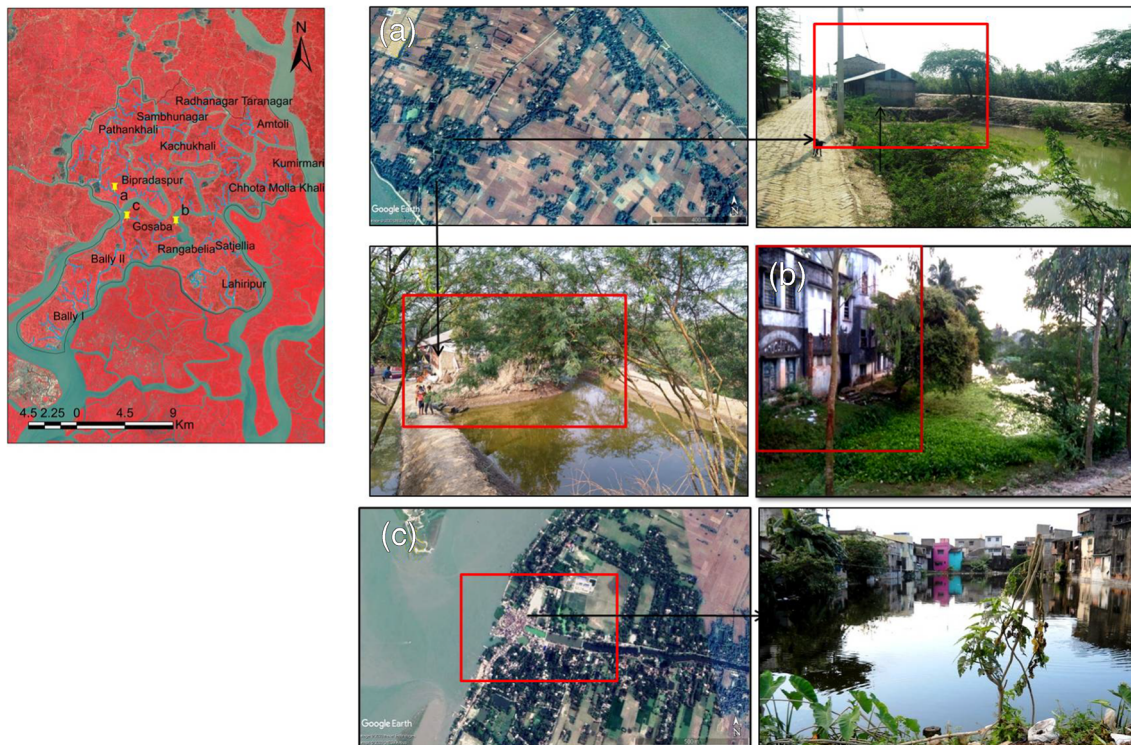


Fig. 9 Anthropogenic interferences on the drainage system (Source: Field photographs collected from (a) Bipradaspur (b) Gosaba (c) Rangabellia during 2017-2018)

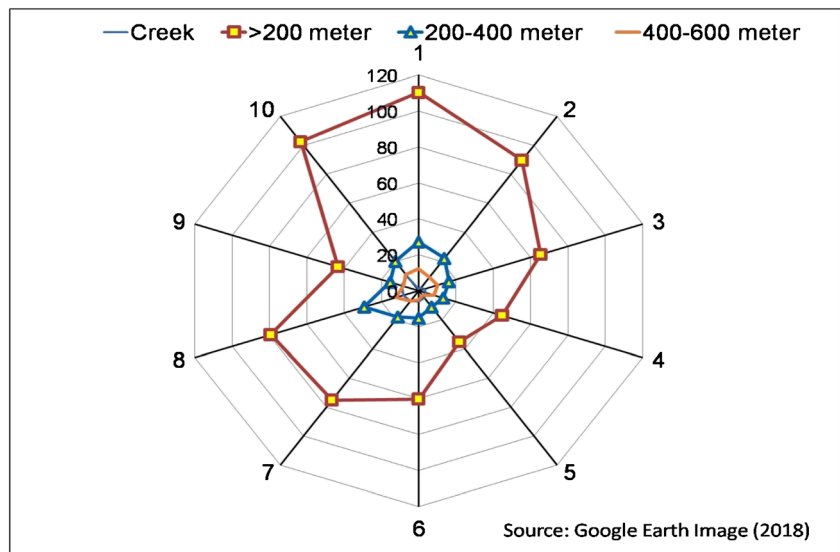
Fig. 12. The severity of this flood may have increased many folds due to a defective drainage system.

Drainage congestion induced waterlogging problem

Waterlogging is a serious challenge for the farmers of this island due to the alteration of gradient and mismanagement of the drainage system. Waterlogging induced by drainage congestion has driven many farmers to monocrop, mainly

paddy cultivation. As the island has a saucer-shaped appearance, prolonged waterlogging occurs in the agricultural fields and sometimes water accumulates even in dry seasons as noted during the survey of the field (Fig. 13). In times of severe weather, farmers face more challenges than usual because of the duration and intensity of waterlogging. During the field investigation, it was observed that the existing lock gate at the creek estuary was not capable enough to drain out the excess water during excessive rainfall in the monsoon season. The

Fig. 10 The proximity of households along the studied creek channels



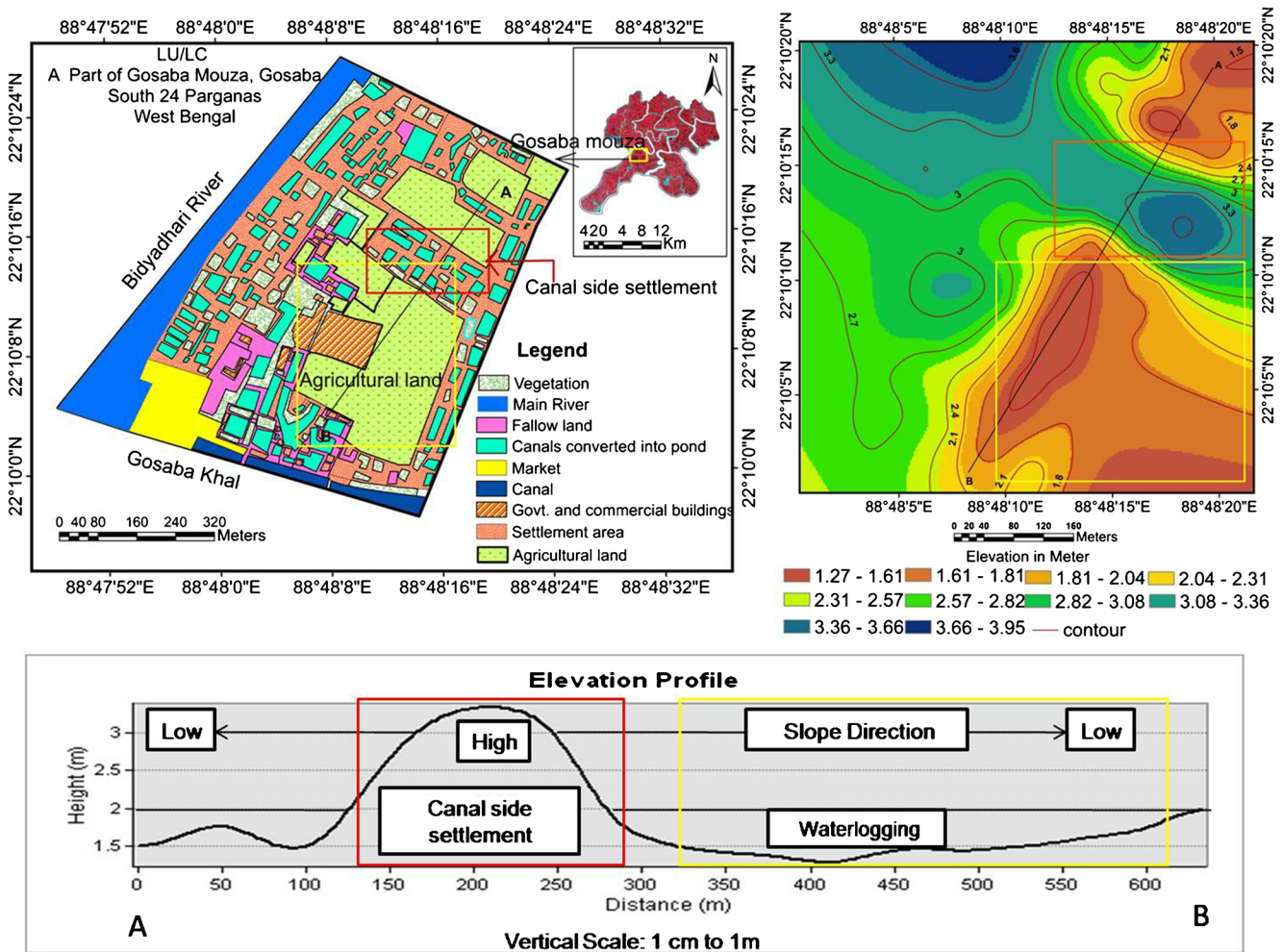


Fig. 11 Change of slope direction with relation to land-use pattern

lack of interconnectivity in the drainage system is contributing to the problem of waterlogging. Farmers suffer a large economic loss because their land potential is not properly utilized.

Conclusions

The morphological change of creek channels at the human-nature interface poses serious threats to coastal environments and the livelihoods of people living in estuaries. The excessive amounts of populations surrounding creeks and the resulting land conversions have changed the surface drainage pattern and the interconnectivity of the drainage channels. The small drainage channels were disconnected from their source river and gradually disappeared from the delta due to the lack of water supply from the source and siltation within the channels. The construction of embankments along creeks and

intermittent obstructions by closures are not only morphologically changed the characteristics of the channels but also altered the gradient of the island. The decay of creek channels and lack of lateral connectivity complicate the management of the water circulation system of the delta. Coastal inundations and waterlogging in agricultural land emerge as a serious threat on this island. The livelihood of local people is extremely dependent on estuarine rivers and drainage channels for agriculture. The inward agricultural land appears as a saucer shape because of the uneven distribution of sediments over the delta. Therefore, farmers are compelled to practice only traditional rice varieties in this waterlogged agricultural land. Moreover, the height of the embankment is not high enough in various places of the island to protect coastal land from storm surges and the resultant floods. Recently, the severity of coastal inundation has been increasing many folds due to the problem of drainage congestion. The mismanagement

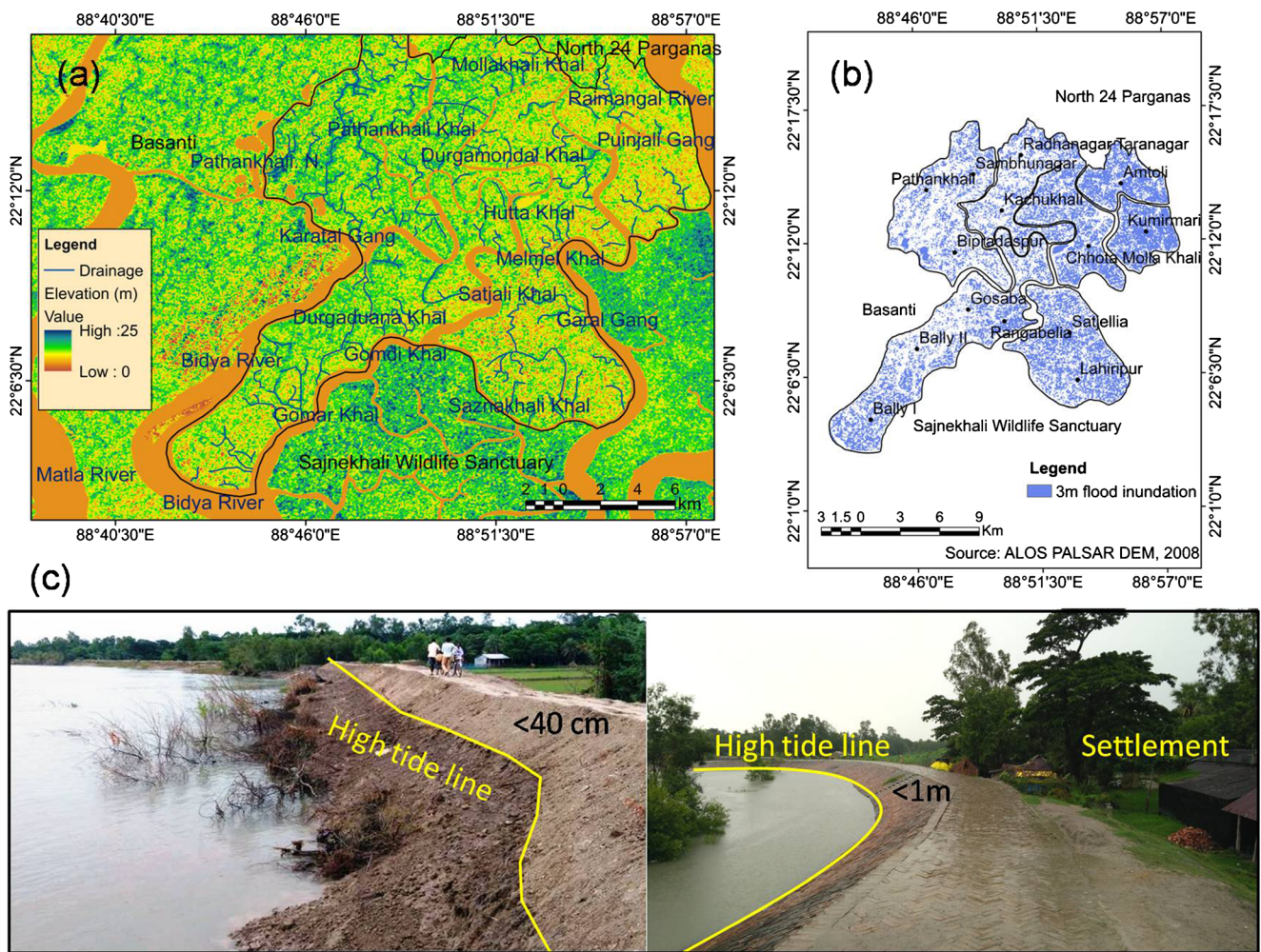
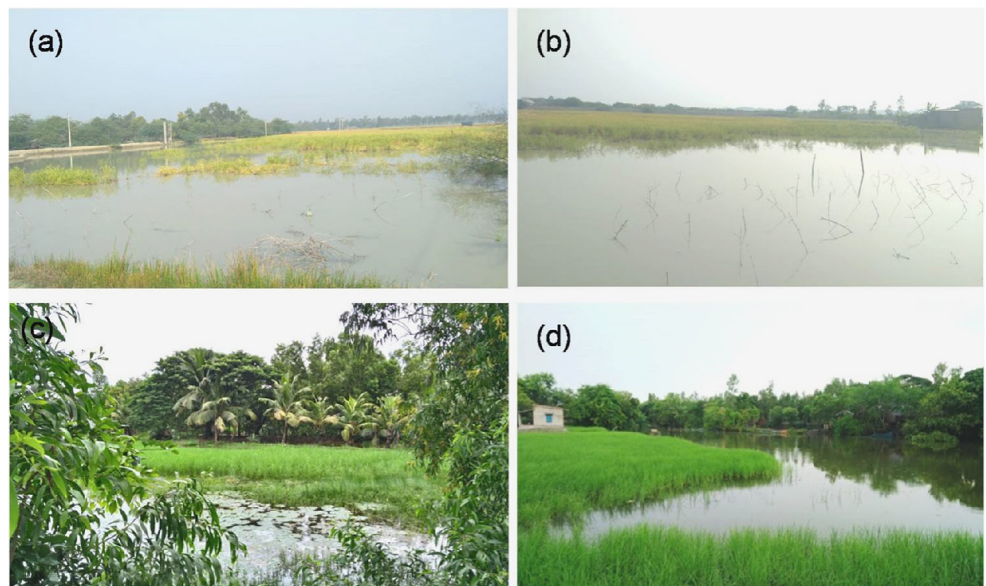


Fig. 12 Risk of flood inundation in Gosaba Island (a) elevation (b) flood inundation (c) height of the embankment from high tide line

of the creek channel is a silent but slow and deadly disaster for the future of coastal residents. To tackle these

coastal challenges, the restoration and protection of the drainage network are of utmost importance in Gosaba

Fig. 13 Waterlogging in agricultural fields (Source: Field photographs collected from (a) & (b) Biradaspur (c) Bally II (d) Rangabellia during 2017-2018)



Island. By restricting imprudent human activities on the drainage system, it is urgently necessary to take some community-centered strategic initiatives to revitalize these decaying creeks.

Acknowledgement The first author is grateful to the University Grants Commission (UGC), New Delhi, India for providing the fellowship to carry out the present work. This work is a part of the M. Phil research work and submitted to the University of Burdwan. The authors are indebted to the whole team for helping in instrumental surveying. The researchers are also thankful to the United States Geological Survey (<https://earthexplorer.usgs.gov/>) for providing free satellite data to pursue this research work.

Declarations

Conflict of Interest The authors declare that they have no conflict of interest

References

- Agrawala S, Ota T, Ahmed AU, Smith J, Van Aalst M (2003) Development and climate change in Bangladesh: focus on coastal flooding and the Sundarbans. OECD, Paris, pp 1–49
- Allison MA (1998) Geological framework and environmental status of the Ganga Brahmaputra Delta. *J. Coast. Res.* 14(2):826–836
- Allison MA, Khan SR, Goodbred SL Jr, Kuehl SA (2003) Stratigraphic evolution of the late Holocene Ganges-Brahmaputra lower delta plain. *Sediment. Geol.* 155(3):317–342. [https://doi.org/10.1016/S0037-0738\(02\)00185-9](https://doi.org/10.1016/S0037-0738(02)00185-9)
- Bandopadhyaya N (1981) 'Operation Barga' and land reforms perspective in West Bengal: a discursive review, *Economic and Political Weekly*, 16(25/26) (Jun. 20–27, 1981), A38–A39
- Bandyopadhyay S, Das S, Kar NS (2021) Avulsion of the Brahmaputra in Bangladesh during the 18th–19th Century: A Review Based on Cartographic and Literary Evidence. *Geomorphology*: 107696.
- Banerjee A (1998) *Environment, Population and Human Settlement*, Concept Publishing Company, 27–32. ISBN: 81-7022-739-9 https://books.google.co.in/books?id=zf_xv9LRd4cC&pg=PA3&source=gbs_selected_pages&cad=3#v=onepage&q&f=false Accessed 02 April 2019
- Bhadra T, Mukhopadhyay A, Hazra S (2017) Identification of river discontinuity using geo-informatics to improve freshwater flow & ecosystem services in Indian Sundarban Delta. In S. Hazra et al. (eds.), *Environment and Earth Observation*. Springer Remote Sensing/Photogrammetry, Switzerland: 137–152. DOI: https://doi.org/10.1007/978-3-319-46010-9_10
- Boesch DF, Turner RE (1984) Dependence of fishery species on salt marshes: the role of food and refuge. *Estuaries* 7(4):460–468
- Brown S, Nicholls RJ (2015) Subsidence and human influences in mega deltas: The case of the Ganges–Brahmaputra–Meghna. *Sci. Total Environ* 527–528:362–374. <https://doi.org/10.1016/j.scitotenv.2015.04.124>
- Census of India (2011) Provisional Population Totals. Registrar General and Census Commissioner of India, Ministry of Home Affairs, New Delhi https://censusindia.gov.in/2011census/dchb/DCHB_A/19/1917_PART_A_DCHB_SOUTH%20TWENTY%20FOUR%20PARGANAS.pdf Assessed 15 March 2019
- Chander G, Markham BL, Helde DL (2009) Summary of current radiometric calibration coefficients for Landsat MSS, TM, ETM+, and EO-1 ALI sensors. *Remote Sens Environ* 113(5):893–903. <https://doi.org/10.1016/j.rse.2009.01.007>
- Church JA, White NJ, Coleman R, Lambeck K, Mitrovica JX (2006) Estimates of the regional distribution of sea-level rise over the 1950 to 2000 period. *J. Clim* 17(13):2609–2625. [https://doi.org/10.1175/1520-0442\(2004\)017<2609:EOTRDO>2.0.CO;2](https://doi.org/10.1175/1520-0442(2004)017<2609:EOTRDO>2.0.CO;2)
- Chust G, Galparsoro I, Borja A, Franco J, Uriarte A (2008) Coastal and estuarine habitat mapping, using LIDAR height and intensity and multi-spectral imagery. *Estuar. Coast. Shelf Sci.* 78:633–643. <https://doi.org/10.1016/j.ecss.2008.02.003>
- Danda AA, Joshi AK, Ghosh A, Saha R (2017) State of art report on biodiversity in Indian Sundarbans. World Wide Fund for Nature-India, New Delhi
- Das A, Agrawal R, Mohan S (2015) Topographic correction of ALOS-PALSAR images using InSAR-derived DEM. *Geocarto Int.* 30(2): 145–153. <https://doi.org/10.1080/10106049.2014.883436>
- Davies G, Woodroffe CD (2010) Tidal estuary width convergence: Theory and form in North Australian estuaries. *Earth Surf. Process. Landf.* 35(7):737–749. <https://doi.org/10.1002/esp.1864>
- Dutta S (2014) Sir Daniel Hamilton and the history of Gosaba. Mitra and Ghosh Publishers, Kolkata, pp 23–35 ISBN: 978-81-7293-996-0
- Fagherazzi S, Kirwan ML, Mudd SM, Guntenspergen GR, Temmerman S, D'Alpaos A, Van de Koppel J, Rybczyk JM, Reyes E, Craft C et al (2012) Numerical models of salt marsh evolution: Ecological, geomorphic, and climatic factors. *Rev. Geophys* 50:1–28. <https://doi.org/10.1029/2011RG000359>
- Federal Geographic Data Committee (FGDC) (USA) (1998). Geospatial positioning accuracy standards. Part 3: national standard for spatial data accuracy. Reston, Virginia, USA. <https://www.fgdc.gov/standards/projects/FGDC-standards-projects/accuracy/part3/chapter3> Accessed 12 December, 2019
- Gayathri R, Prasad KB, Sen D (2015) Numerical study on Storm Surge and associated coastal inundation for 2009 AILA Cyclone in the head Bay of Bengal. *Aquat. Procedia* 4:404–411. <https://doi.org/10.1016/j.aqpro.2015.02.054>
- Ghosh S, Mistri B (2020a) Geo-historical appraisal of embankment breaching and its management on active tidal land of Sundarban: a case study in Gosaba Island, South 24 Parganas, West Bengal. *Space and Culture India* 7(4):166–180. <https://doi.org/10.20896/saci.v7i4.587>
- Ghosh S, Mistri B (2020b) Spatio-temporal change of drainage network at human-nature interface and its future implication to the estuarine environment in Gosaba Island, Sundarban, India. *Geogr. Environ. Sustain.* 13(4):148–158
- Ghosh S, Mistri B (2020c) Drainage induced waterlogging problem and its impact on farming system: a study in Gosaba Island, Sundarban, India. *Spatial Information Research* 28(6):709–721
- Ghosh A, Mukhopadhyay S (2016) Quantitative study on shoreline changes and erosion hazard assessment: case study in Muriganga–Saptamukhi interfluvium, Sundarban, India. *Model Earth Syst Environ* 2(75):1–14. <https://doi.org/10.1007/s40808-016-0130-x>
- Ghosh A, Schmidt S, Fickert T, Nusser (2015) The Indian Sundarban mangrove forests: history, utilization, conservation strategies and local perception. *Diversity* 7:149–169. <https://doi.org/10.3390/d7020149>
- Goodbred SL Jr, Kuehl SA (2000) The significance of large sediment supply, active tectonism and eustasy on margin sequence development: Late Quaternary stratigraphy and evolution of the Ganges-Brahmaputra Delta. *Sediment. Geol.* 133(3–4):227–248. [https://doi.org/10.1016/S0037-0738\(00\)00041-5](https://doi.org/10.1016/S0037-0738(00)00041-5)
- Gopinath G, Seralathan P (2005) Rapid erosion of the coast of Sagar island, West Bengal-India. *Environmental Geology* 48(8):1058–1067
- Halder A, Debnath A (2014) Assessment of climate induced soil salinity conditions of Gosaba Island, West Bengal and its influence on local livelihood. In M. Singh et al. (eds.), *Climate Change and*

- Biodiversity: Proceedings of IGU Rohtak Conference, 1, Advances in Geographical and Environmental Sciences, 27-44 DOI: https://doi.org/10.1007/978-4-431-54838-6_3
- Hazra S, Ghosh T, DasGupta R, Sen G (2002) Sea Level and associated changes in the Sundarbans. *Science and Culture* 68(9):309–321
- Holgate SJ, Woodworth PL (2004) Evidence for enhanced coastal sea level rise during the 1990s. *Geophys. Res. Lett.* 31(7):1–4. <https://doi.org/10.1029/2004GL019626>
- Hood WG (2010) Tidal channel meander formation by depositional rather than erosional processes: Examples from the prograding Skagit River Delta (Washington, USA). *Earth Surf. Process. Landf.* 35(3): 319–330. <https://doi.org/10.1002/esp.1920>
- Ijaz MW, Mahar RB, Siyal AA, Anjum MN (2018) Geospatial analysis of creeks evolution in the Indus Delta, Pakistan using multi sensor satellite data. *Estuar. Coast. Shelf Sci.* 200:324–334. <https://doi.org/10.1016/j.ecss.2017.11.025>
- Islam MJ, Alam MS, Elahi KM (1997) Remote Sensing for Change Detection in the Sundarbans, Bangladesh. *Journal of Geocarto International* 12(3):91–10. <https://doi.org/10.1080/10106049709354601>
- Jana A, Biswas A, Maiti S, Bhattacharya K (2013) Shoreline changes in response to sea level rise along Digha Coast, Eastern India: an analytical approach of remote sensing, GIS and statistical techniques. *J. Coast. Conserv.* 17(4):72–81. <https://doi.org/10.1007/s11852-013-0297-5>
- Ji L, Zhang L, Wylie B (2009) Analysis of dynamic thresholds for the normalized difference water index. *Photogrammetric Engineering & Remote Sensing* 75(11):1307–1317
- Kar NS, Bandyopadhyay S (2015) Tropical storm Aila in Gosaba Block of Indian Sundarban: remote sensing based assessment of impact and recovery. *Geogr Rev India* 77(1):40–54
- Khan TMA, Singh OP, Rahman MS (2000) Recent sea level and sea surface temperature trends along the Bangladesh coast in relation to the frequency of intense cyclones. *Mar. Geod.* 23(2):103–116
- Kim D, Cairns DM, Bartholdy J (2013) Tidal creek morphology and sediment type influence spatial trends in salt marsh vegetation. *Prof Geogr* 65(4):544–560
- Leopold LB, Wolman MG (1957) River channel patterns, braided, meandering and straight. *U.S. Geol. Surv. Paper.* 282-B
- Li W, Du Z, Ling F, Zhou D, Wang H, Gui Y, Sun B, Zhang X (2013) A Comparison of land surface water mapping using the normalized difference water index from TM, ETM+ and ALI. *Remote Sensing* 5(11):5530–5549. <https://doi.org/10.3390/rs5115530>
- Liu YX, Li MC, Mao L, Cheng L, Chen KF (2013) Seasonal pattern of tidal-flat topography along the Jiangsu Middle Coast, China, Using HJ-1 Optical Images. *Wetlands* 33:871–886
- Marani M, Belluco E, D’Alpaos A, Defina A, Lanzoni S, Rinaldo A (2003) On the drainage density of tidal networks. *Water Resour. Res.* 39(2):1040. <https://doi.org/10.1029/2001WR001051>
- McSweeney SL, Kennedy DM, Rutherford ID (2017) A geomorphic classification of intermittently open/closed estuaries (IOCE) derived from estuaries in Victoria, Australia. *Progress in Physical Geography SAGE* 20(10):1–29. <https://doi.org/10.1177/0309133317709745>
- Mistri B (2014) Construction of closure on tidal creeks and its effects: a case study of Pathar Pratima CD Block of sundarban. *Nature and Sustainable Development-Impact of Green Accounting*, Published by Academic Staff College, The University of Burdwan, 111-124
- Novakowski KI, Torres R, Gardner LR, Voulgaris G (2004) Geomorphic analysis of tidal creek networks. *Water Resour. Res.* 40(5):1–13. <https://doi.org/10.1029/2003WR002722>
- O’Mally LSS (1914) *Rivers of Bengal*, Bengal District Gazetteers. The Bengal Secretariat Book Depot
- Pargiter FE (1934) *A Revenue History of the Sundarbans from 1765 to 1870*. Bengal Government Press, Calcutta
- Pavlis NK, Holmes SA, Kenyon SC, Factor JK (2012) The development and evaluation of the Earth Gravitational Model 2008 (EGM 2008). *J. Geophys. Res.* 117(B4):B04406
- Rahman MM, Ghosh T, Salehin M, Ghosh A, Haque A, Hossain MA., ..., Hutton CW (2020) Ganges-Brahmaputra-Meghna delta, Bangladesh and India: a transnational mega-delta. In *Deltas in the Anthropocene* (pp. 23-51). Palgrave Macmillan, Cham
- Rogers KG, Steven LG Jr (2014) The Sundarban and Bengal Delta: the world’s largest tidal mangrove and delta system. In: Kale VS (ed) *Landscapes and Landforms of India*. Springer, New York, pp 1–12. https://doi.org/10.1007/978-94-017-8029-2_18
- Rudra K (2016) State of India’s River for India’s River Week, A consortium of organizations comprising WWF-India, SANDRP, Toxics Link, INTACH and PEACE Institute under the guidance of Late Sri Ramaswamy Iyer, initiated the India Rivers Week
- Sakib M, Nihal F, Haque A, Rahman M, Ali M (2015) Sundarban as a buffer against storm surge flooding. *World Journal of Engineering and Technology* 3:59–64
- Sánchez-Triana E, Ortolano L, Paul T (2018) Managing water-related risks in the West Bengal Sundarbans: policy alternatives and institutions. *Int J Water Resour Dev.* 34(1):78–96. <https://doi.org/10.1080/07900627.2016.1202099>
- Sanyal P (1999) Global warming in Sundarban delta and Bengal Coast. In: Guha Bakshi DN, Sanyal P, Naskar KR (eds) . *Sundarbans Mangal- Naya Prokash*, Kolkata
- Sarkar H, Roy A, Siddique G (2016) Impact of embankment breaching and rural livelihood: A case Study in Ghoramara Island of the Sundarbans Delta in South 24 Parganas. *The Journal of Bengal Geographer* 5(4):97–117
- Seminara G, Lanzoni S, Tambroni N, Toffolon M (2010) How long are tidal channels? *J. Fluid Mech* 643:479–494. <https://doi.org/10.1017/S0022112009992308>
- Shi Z, Lamb HF, Collin RL (1995) Geomorphic change of salt-marsh tidal creek networks in the DYFI Estuary. *Wales. Mar. Geol.* 128: 73–83
- Stefanon L, Carniello L, D’Alpaos A, Lanzoni S (2010) Experimental analysis of tidal network growth and development. *Cont. Shelf Res.* 30(8):950–962. <https://doi.org/10.1016/j.csr.2009.08.018>
- Tambroni N, Pittaluga MB, Seminara G (2005) Laboratory observations of the morphodynamic evolution of tidal channels and tidal inlets. *J. Geophys. Res. Earth Surf.* 110(F4):1–19. <https://doi.org/10.1029/2004JF000243>
- Williams PB, Orr MK, Garrity NJ (2002) Hydraulic geometry: a geomorphic design tool for tidal marsh channel evolution in wetland restoration projects. *Restor. Ecol.* 10(3):577–590. <https://doi.org/10.1046/j.1526-100X.2002.t01-1-02035.x>
- Xu H (2006) Modification of normalized difference water index (NDWI) to enhance open water features in remotely sensed imagery. *Int. J. Remote Sens.* 27:3025–3033
- Zhao B, Liu Y, Xu W, Liu Y, Sun J, Wang L (2019) Morphological characteristics of tidal creeks in the Central Coastal Region of Jiangsu, China, Using LiDAR. *Remote Sens.* 11(2426):1–19. <https://doi.org/10.3390/rs11202426>